iScience

Article

Blocking CCL3-mediated neutrophil recruitment into the brain alleviates immunopathology following severe enterovirus 71 infection

Graphical abstract

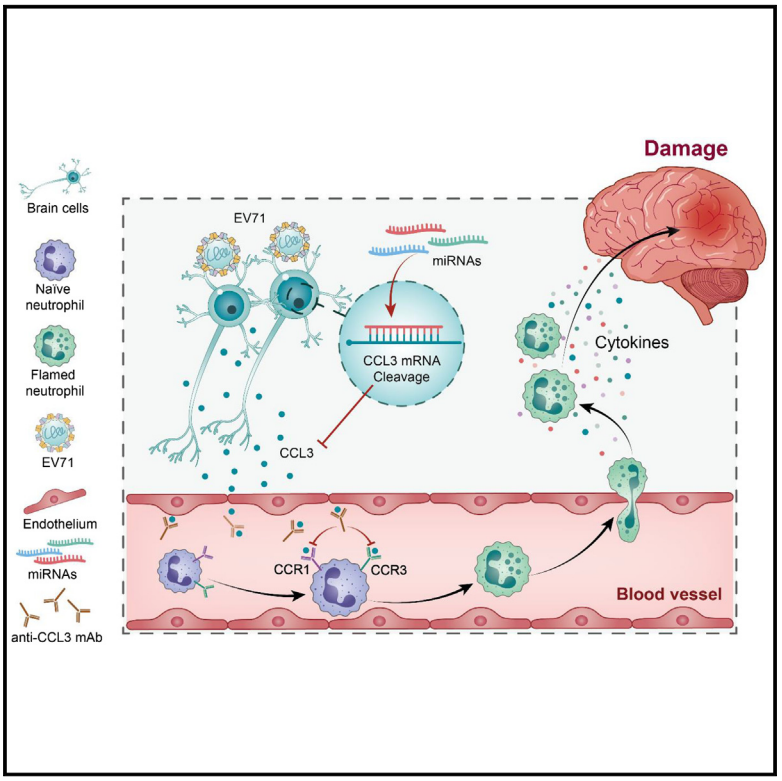

Highlights

- Neutrophils play a pivotal role in EV71-induced fatal immunopathology
- CCL-3 was identified as the key chemokine for recruiting neutrophils during EV71 infection
- CCL3 recruit neutrophils into the brain through CCR1/3(human)/CCR5(mouse)

Authors

Wenxian Yang, Li Li, Guanlin Li, ..., Guangyu Zhao, Lei Sun, Min Li

Correspondence

gb5029@hotmail.com (B.G.), zhaoguangyu0525@outlook.com (G.Z.), sunlei362@im.ac.cn (L.S.), luckylixiaomi@163.com (M.L.)

In brief

Immunology; Clinical neuroscience; Virology

Yang et al., 2024, iScience 27, 111388
December 20, 2024
https://doi.org/10.1016/j.isci.2024.111388

CellPress

iScience

CellPress
OPEN ACCESS

Article

Blocking CCL3-mediated neutrophil recruitment into the brain alleviates immunopathology following severe enterovirus 71 infection

Wenxian Yang,[2,8] Li Li,[3,8] Guanlin Li,[5,6,8] Xiuhui Li,[3] Hongyan Liu,[7] Xuelian Han,[1] Yuan Wang,[1] Yali Sun,[1] Yuwei Wei,[1] Bo Gao,[4,*] Guangyu Zhao,[1,*] Lei Sun,[2,*] and Min Li[1,9,*]

[1]State Key Laboratory of Pathogen and Biosecurity, Academy of Military Medical Sciences, Beijing 100071, China
[2]CAS Key Laboratory of Pathogenic Microbiology and Immunology, Institute of Microbiology, Chinese Academy of Sciences, Beijing 100101, China
[3]You'an Hospital, Capital Medical University, Beijing, Fengtai 100069, China
[4]Beijing Institute of Basic Medical Sciences, 27 Taiping Road, Beijing 100850, China
[5]Associate Chief Technician, Department of Clinical Laboratory, The First Affiliated Hospital of Zhengzhou University, Zhengzhou, China
[6]Key Clinical Laboratory of Henan Province, Zhengzhou, China
[7]Shenyang Infectious Diseases Hospital, Shenyang, Liaoning Province, China
[8]These authors contributed equally
[9]Lead contact
*Correspondence: gb5029@hotmail.com (B.G.), zhaoguangyu0525@outlook.com (G.Z.), sunlei362@im.ac.cn (L.S.), luckylixiaomi@163.com (M.L.)
https://doi.org/10.1016/j.isci.2024.111388

SUMMARY

Inflammatory cells infiltration in the cerebrospinal fluid is a hallmark of severe enterovirus 71 (EV71) infection, but which type of immune cells are critical for severe EV71 infection remains unclear. Here, we observe that both neutrophils and macrophages are increased in the brains of patients and mice with severe EV71 infection, and the depletion of neutrophils but not macrophages results in a marked enhancement of survival of EV71-infected mice. Furthermore, CCR1/3 may play an important role in CCL3 facilitating the accumulation of neutrophils in the brains of patients. Inhibition of CCL3 by anti-CCL3 antibodies or selected miRNAs significantly reduces the neutrophils infiltration in brains and the mortality of EV71-infected mice. Collectively, CCL3-mediated neutrophils recruitment into the brain contributes to the severe immunopathology of EV71 infection, which provides a potential diagnostic and therapeutic target for EV71 infection.

INTRODUCTION

Enterovirus infection represents an ongoing serious health concern. Infection with enterovirus 71 (EV71), in particular, occasionally causes pulmonary dysfunctions and many other neurologic manifestations[1], resulting in a clinical syndrome of hand, foot, and mouth disease (HFMD) and herpangina in children. In most cases the disease is mild and self-limiting, but it can lead to severe symptoms with prolonged illnesses such as aseptic meningitis, acute generalized flaccid paralysis, and encephalitis. Encephalitis may affect the brainstem, leading to severe neurogenic-induced pulmonary edema (PE) and severe cardiorespiratory symptoms[2]. Consecutive epidemics of EV71 infection in the Asia-Pacific region in recent years are a matter of growing concern in the affected countries as well as on a global level. Focused efforts in the infectious disease heath sector, however, has yet to yield any specific or effective treatment for this infectious agent and its associated diseases.[3] Development of efficacious therapeutic against EV71 remains an urgent need, which unfortunately cannot be met until a clearer understanding of the interactive mechanisms of the host immune system is attained.

EV71 is a neurotropic virus belonging to the *Enterovirus A* species of the *Enterovirus* genus of the family *Picornaviridae*. EV71-mediated effects on the host immune system, particularly on promotion of inflammation in the central nervous system (CNS), are likely important contributors to the neural disorders associated with this infectious disease. Severe inflammation can occur in various regions of the CNS system upon EV71 infection, including the cerebral cortex, brainstem, and all levels of the spinal cord. The detection of EV71 viral genomes and antigens, as well as virus-like particles and inclusions, in neurons as well as inflammatory cells at the focus of infection[4,5] further suggests a correlation between neural inflammation and EV71 infection. Reported cases of EV71 infection fatalities related to PE or hemorrhage[6,7] have shown inflammation localized to the spinal cord and the brain. For cases of EV71-induced encephalitis, it has been theorized that the associated pulmonary and cardiovascular decompensation may result from EV71-induced damage to the medullary vasomotor centers.[8] Intriguingly, patients with EV71-associated PE lack detectable levels of either viral particles or inflammation in the lung and heart.[8] These observations support that the notion that EV71 PE is neurogenic. Contribution

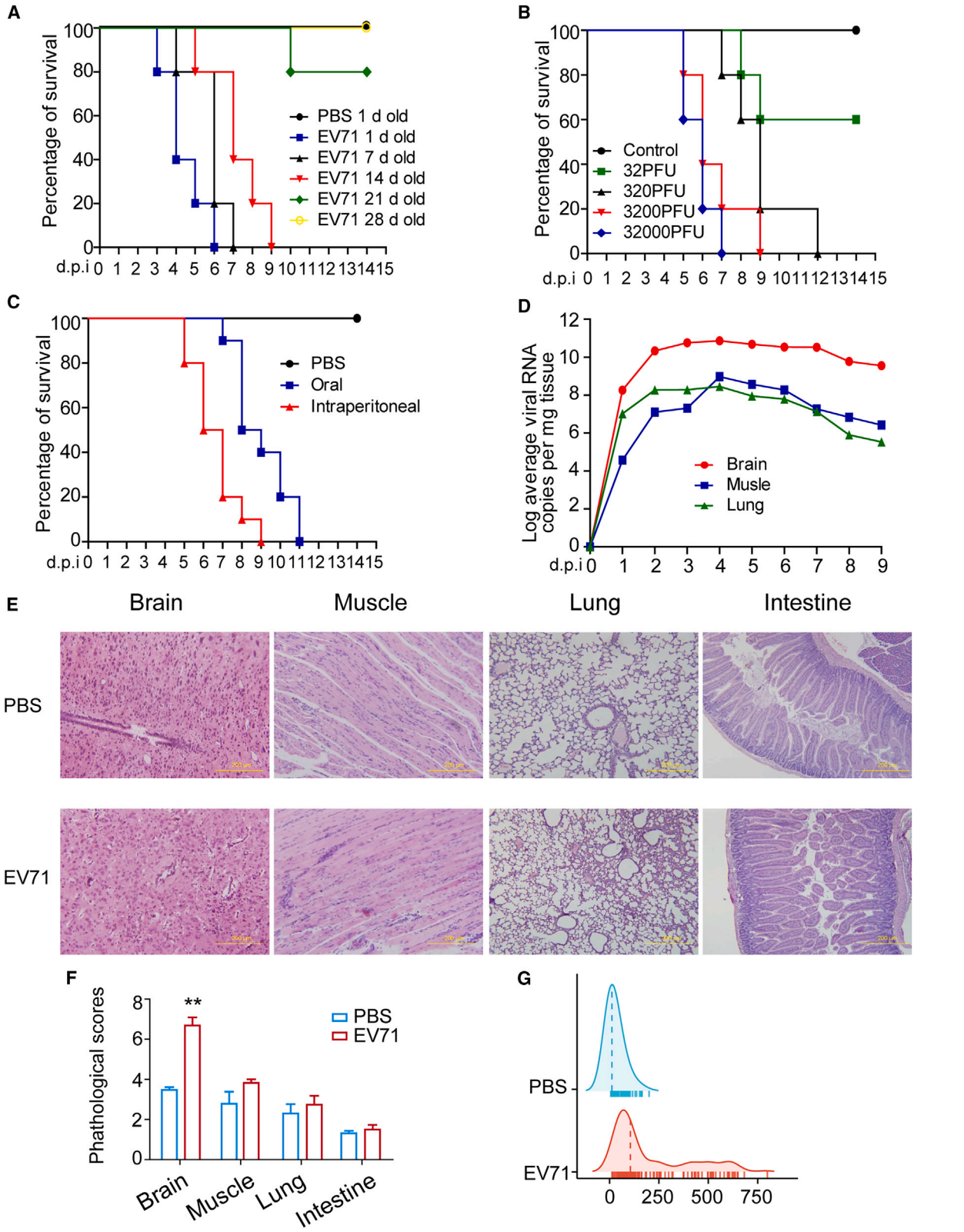

(legend on next page)

of EV71-induced inflammation in the CNS to development of encephalitis, aseptic meningitis, and brainstem encephalitis, highlights the possibility that EV71-associated systemic inflammatory and immune responses lead to severe EV71-related diseases.

Both innate and adaptive immune responses contribute to inflammation. Patients with EV71 infection show remarkably elevated levels of proinflammatory factors, including the cytokines IL-6, TNF-α, IL-1β, IL-8, INF-γ-induced protein (IP)-10, the chemokines monocyte chemoattractant protein (MCP)-1, and monokine induced by INF-γ (MIG).[9,10] However, these patients also show increased white blood cell (WBC) counts[11,12] and decreased amounts of natural killer (NK) cells, $CD4^+$, and $CD8^+$T-lymphocytes.[12] One study of EV71-infected Chinese patients also showed a large amount of neutrophil-like inflammatory cells, consisting of $CD68^+$ and $CD15^-$ cells mostly, which had infiltrated into CNS regions[5]. Thus, the innate immune response might play a pivotal role in EV71 infection progressing to a severe status. However, which type of immune cells is critical for severe EV71 infection remains unclear.

In this study, we find that the recruitment of neutrophils into the brain contributes to the severe immunopathology of EV71 infection and CCL3 involves in this process. These results represent potential diagnostic and therapeutic targets for addressing and resolving critical EV71 infection.

RESULTS

EV71 infection led to extensive peripheral and CNS inflammatory responses in mice

To establish a mouse model of severe EV71 infection, the mouse age (Figure 1A), virus dose (Figure 1B), and route of inoculation (Figure 1C) were investigated by evaluating the survival of mice. As a result, the 14-day-old C57BL/6 mice were injected i.p. with EV71 TS stain (GenBank No. JQ708210.1) isolated from human (3200 PFU/mouse, 100 LD_{50}). The virus was localized primarily to the brain tissues, with much less extensive but detectable levels in muscle and lung tissues (Figure 1D). The severe inflammation occurred in brain tissues, and mild inflammation occurred in muscle, lung, and intestinal tissues (Figures 1E and 1F). Sharply increased cytokines and chemokines were observed in sera from the EV71-infected mice (Figures 1G and S1). Together, the severe EV71-infected mice model exhibits extensive peripheral and CNS inflammatory responses, which is similar to the clinical feature of critical patients of EV71 infection.

Neutrophils infiltration in brain contributes to EV71-induced fatal immunopathology in patients and mice

Death in the EV71-infected patients usually occurred after a week post-infection in patients and mice. It has been reported that leukocytosis plays a crucial role in patients with fatal EV71 infection, but the detailed mechanism is still unknown.[12] To investigate which type of leukocytosis are crucial to the fatal pathogenesis of EV71 infection, we examined the leukocytes in the peripheral blood and the CSF/brain of EV71-infected patients and mice. The peripheral blood samples from critical patients with severe EV71 infection showed no significantly change in either total leukocyte count or monocyte count (Figure 2A), compared to controls, but markedly higher frequency of neutrophils (CD45) and sharply lower frequency of lymphocytes were noted (Figure 2B). Compared to controls, the CSF samples from critical patients showed significantly higher total leukocyte count (Figure 2C) and neutrophil frequency, but comparable frequency of monocyte (CD45) and lymphocyte counts, although there was a higher level of activated monocyte in the critical patients (Figure 2D). The FCM analysis of the brain-infiltrated leukocytes of the EV71-infected mouse demonstrated that there were markedly increased neutrophils and activated monocytes (macrophages) but sharply decreased microglia cells (Figure 2E). The frequencies of other immune cell types fluctuated only slightly following the EV71 infection (Figure 2E). In addition, the EV71-infected *Rag1*$^{-/-}$ mice, which lack mature functional T and B cells, were all dead after about 7 dpi, indicating that innate immunity rather than adaptive immunity is responsible for EV71-induced death (Figures S2A and S2B). There results indicate that the neutrophils and macrophages appeared to contribute to the fatal pathogenesis of EV71 infection.

We then sought to determine whether the markedly increased neutrophils and macrophages both mediate the fatal pathogenesis of EV71 infection in the mouse model. Neutrophil depletion by i.p. injection of 1A8 antibody (Figure 2F) and macrophage depletion by i.p. injection of gadolinium (III) chloride hexahydrate (Figure S3A) led to marked decreases of the respective cell types in brain tissues upon infection with EV71. The neutrophil depletion led to significantly enhanced survival (Figure 2G)

Figure 1. Establishment of the mouse model of severe EV71 infection

(A) Inoculation of EV71 results in age-dependent mortality. C57BL/6 mice (n = 5 per age) were inoculated i.p. with EV71 (3200 PFU/mouse) at 1, 7, 14, 21 or 28 days of age. Mortality was monitored and recorded daily after infection. Representative results of three independent experiments are shown.

(B) Inoculation of EV71 results in dose-related mortality. 14-day-old C57BL/6 mice (n = 5 per group) were inoculated i.p. with increasing dosages of EV71 (32, 320, 3200 and 32000 PFU/mouse). Control animals were given PBS instead of EV71. Mortality was monitored and recorded daily after infection. A representative result of three independent experiments is shown.

(C) Survival rates of C57BL/6 mice infected with100LD50/mouse of EV71. 14-day-old C57BL/6 mice (n = 10 per group) were infected i.p. or orally. Control mice received PBS instead of EV71. Survival was monitored daily. Representative results of three independent experiments are shown.

(D) Dynamics of EV71 replication in 14-day-old C57BL/6 mice infected i.p. with 100LD50/100 μL/mouse EV71. EV71 virion numbers in the brain, muscle and lung were determined by qRT-PCR.

(E) Histology (HE-stained) of infected mice after i.p. challenge with lethal doses of EV71. 14-day-old C57BL/6 mice were inoculated i.p. with PBS or EV71 (100LD50). Representative results at 6 days post-infection are shown.

(F) Pathological scores of (E).

(G) Density distribution of 23 cytokines fold change of PBS (green), EV71(red)/PBS, in the sera of EV71-infected mice. Data are representative of three independent experiments. Data are reported as the mean ± SD, n = 6. *$p < 0.05$ and **$p < 0.01$ (unpaired, two-tailed Student's t test).

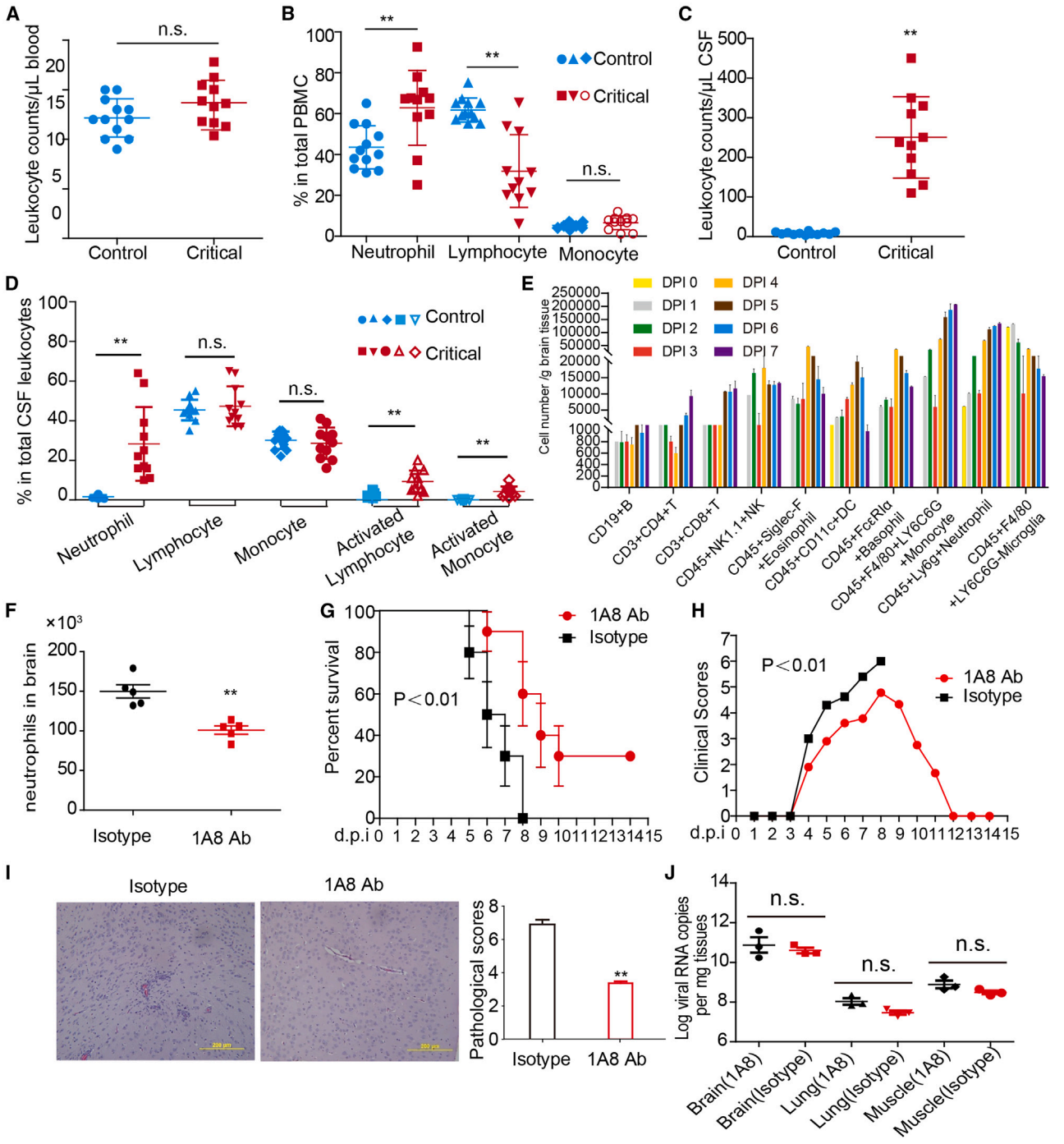

Figure 2. Neutrophils infiltration in brain contributes to EV71-induced fatal immunopathology in patients and mice

(A and B) Leukocyte count (A) and percentage of leukocyte subtypes(B) in human PBMCs.

(C and D) Leukocyte count (C) and percentage of leukocyte subtypes(D) in human CSF.

(E) A dynamic analysis of cell counts of the indicated leukocyte subtypes in brain tissues of EV71-infected mice (100LD_{50}/100 μL/mouse of EV71).

(F) EV71-infected mice (100LD_{50}/100 μL/mouse of EV71) were injected i.p. with anti-Ly6G mAb (1A8) antibody (100 μg/100 μL/mouse) on 1, 3 and 5 dpi; for controls, the respective isotype antibodies were injected using the same protocol. FCM analysis the neutrophils in brain at 6 dpi.

(G and H) The mortality (G)and clinical scores (H) of mice in (F) were monitored and recorded daily after infection.

(I) HE staining and the pathological scores of brain tissues of mice in (F).

(J) qRT-PCR analysis the EV71 RNA copy number in brain, lung and muscle of mice in (F).Data are representative of three independent experiments. Data are reported as the mean ± SD, $n = 6$. *$p < 0.05$ and **$p < 0.01$ (unpaired, two-tailed Student's t test).

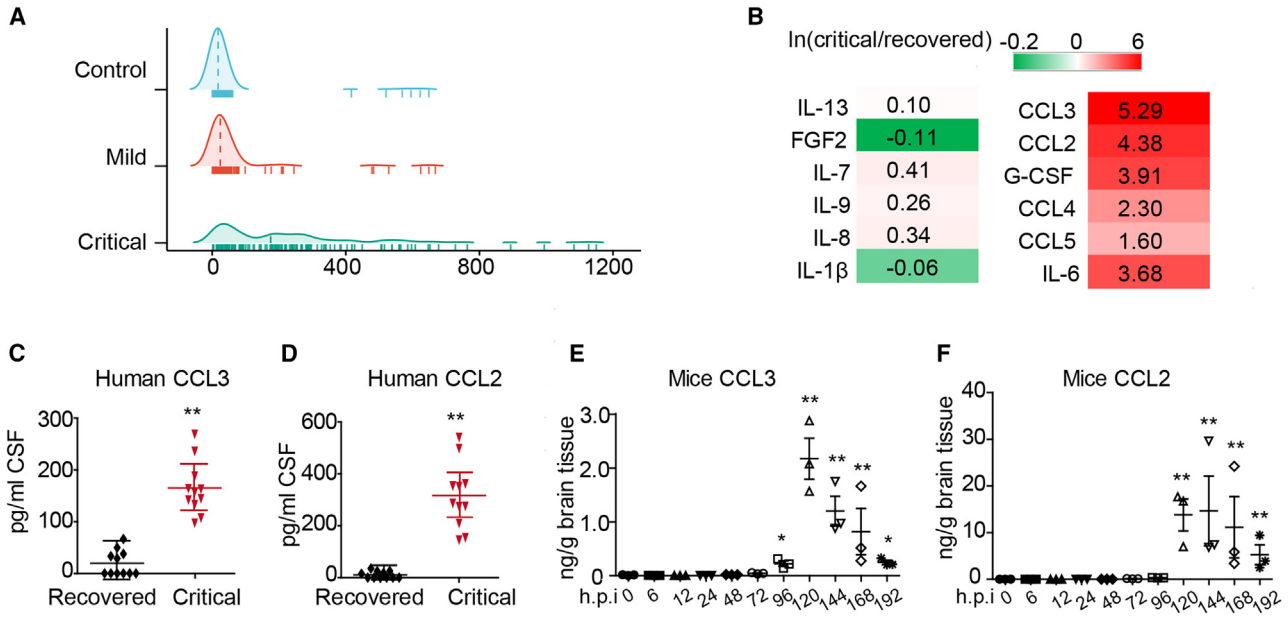

Figure 3. CCL3 and CCL2 showed the most robust increases in CSF of patients and mice during severe EV71 infection

(A) Density distribution of 27 cytokines fold change of control (red), mild (blue) or critical (green)/control, in the sera of EV71-infected patients.

(B) QPCR analysis of cytokines fold changes of critical/recovered CSF of patients.

(C and D) CCL3 (C) and CCL2 (D) protein levels in CSF of patients with EV71 and brainstem encephalitis (severe immunopathology) at either the acute phase or recovery phase, measured by ELISA.

(E and F) CCL3 (E) and CCL2 (F) protein levels in brain tissues of EV71-infected mice, measured by ELISA. Data are representative of three independent experiments. Data are reported as the mean ± SD, $n = 10$. *$p < 0.05$ and **$p < 0.01$ vs isotype antibody or WT mice (unpaired, two-tailed Student's t test).

and reduced clinical scores (Figure 2H), while the macrophage depletion appeared to have no effect (Figures S1B and S1C). The neutrophil depletion was also associated with significantly ameliorated inflammation in the brain tissues (Figure 2I), but the macrophage depletion appeared to have no effect (Figure S1D). In addition, it did not show any effect on the viral load in either the brain, lung, or muscle (Figure 2J). Thus, neutrophils infiltration in brain appears to be the main effector involved in the robust immunopathogenesis induced by EV71 infection.

CCL3 and CCL2 are robustly increased in CSF of patients and mice during severe EV71 infection

To elucidate which factor(s) chemoattract the neutrophils to the brain tissues during severe EV71 infection, we performed Luminex assay to examine the differential profiles of cytokines and chemokines in sera and CFS of EV71-infected patients compared to controls. Elevated levels of cytokines and chemokines, including the chemokines for neutrophils such as CCL2 (MCP1), CCL3 (MIP-1α), IL-8, CXCL-1/KC, and CXCL-10/IP-10 were observed in sera from EV71-infected patients (Figures 3A and S4), and the levels of CCL2, CCL3, CCL4, CCL5, IL-6, and G-CSF were significantly increased in CSF of critical patients as compared with the patients who recovered from EV71 infection (Figure 3B). Among these chemokines, CCL3 and CCL2 showed the most robust increases. The ELISA results also showed that both CCL3 and CCL2 were significantly increased in the CSF from the critical EV71-infected patients (Figures 3C and 3D). Similar changes in cytokines and chemokines levels were observed in sera (Figure S1) and brain tissues (Figures 3E and 3F) (corresponding to the results of the human CSF samples) of EV71-infected mice, with peak levels occurring at 5–6 dpi. It is suggested that CCL2 and CCL3 could be the major chemokines for recruiting neutrophils into the brains of EV71-infected mice.

CCL3 but not CCL2 deletion reduces neutrophils infiltration in brain and mortality of severe EV71-infected mice

To further verify the roles of CCL3 and CCL2 in neutrophils infiltration and fatal immunopathogenesis during severe EV71 infection, the C57BL/6 mice with CCL3 and CCL2 knocked-out were infected with EV71. FCM assay demonstrated that CCL3 KO mice had significantly decreased neutrophils in brain tissues in response to EV71 infection, compared to control mice. In contrast, the CCL2 KO mice did not show a remarkable difference in accumulated neutrophils in brain tissues as compared with the control mice (Figures 4A and 4B). IF staining also demonstrated that CCL3 deletion prevented neutrophil accumulation in the cerebral ventricles following EV71 infection while the CCL2 deletion provided no such protection (Figures 4C and 4D). Morphological assessment by HE staining showed that, unlike CCL2 KO, CCL3 KO effectively protected mice from severe damage in brain tissues (Figures 4E and 4F). Compared to the 100% rate of death within 1 week among the wild-type (WT) control mice and CCL2 KO mice, ~60% of the CCL3 KO mice survived through 2 weeks post-infection (Figure 4G). The clinical scores (Figure 4H) and infection-related changes in average body

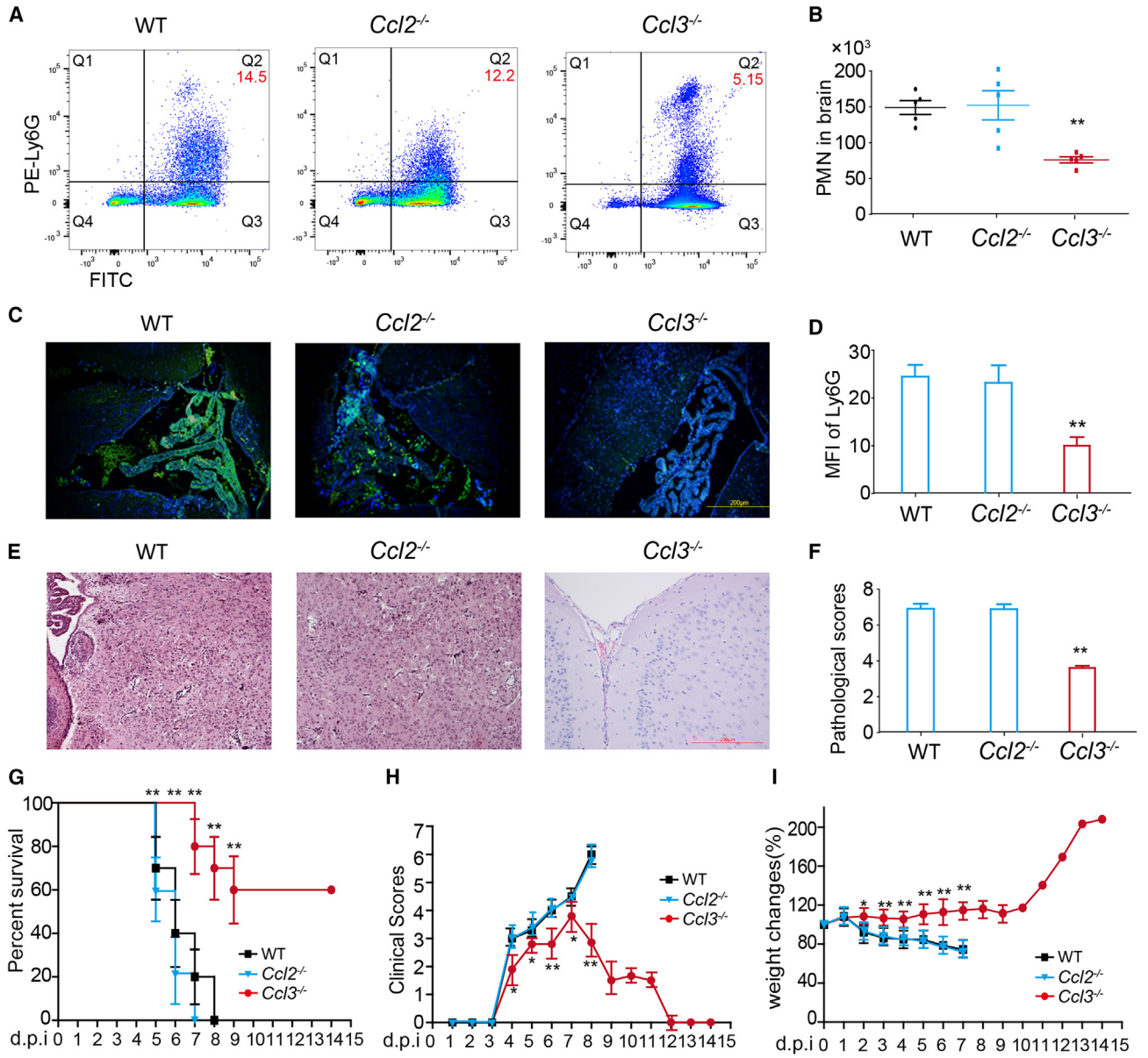

Figure 4. The deficiency of CCL3 reduces neutrophils infiltration in brain and mortality of severe EV71-infected mice

2 weeks old WT, *Ccl3*$^{-/-}$ and *Ccl2*$^{-/-}$ C57BL/6 mice were injected i.p. with 100LD50/100 μL/mouse of EV71.

(A and B) Leukocytes were isolated from brain tissues by Ficoll Reagent and stained with anti-CD45-FITC and anti-Ly6G-PE on day 6 dpi. The percentages of neutrophils (CD45^{+}Ly6G^{+}) in total leukocytes were detected by FCM assay (A) and the corresponding statistical analyses are shown (B).

(C and D) Immunofluorescence histochemistry analysis Ly6G for neutrophils in brain tissues (C) and the mean fluorescence intensity (MFI) (D) on day 6 dpi.

(E and F) HE staining (E) and pathological scores of brain tissues (F) on day 6 dpi.

(G–I) The mortality (G), body weight (H) and clinical scores (I) of mice (A) were monitored and recorded daily after infection. Data are representative of three independent experiments. Data are reported as the mean ± SD, $n = 10$. *$p < 0.05$ and **$p < 0.01$ vs isotype antibody or WT mice (unpaired, two-tailed Student's *t* test).

weights (Figure 4I) were in concordance with the survival rate. Additionally, the transwell assays showed that CCL3 was able to chemoattract neutrophils markedly, while CCL2 and the positive control fMLP chemoattracted neutrophils mildly (Figure 5A). These results suggest that CCL3 but not CCL2 mediates neutrophils infiltration in brain and fatal immunopathogenesis of EV71 infected mice.

mRNA expression of CCR1/3(human)CCR5(mouse) were upregulated during severe EV71 infection

We next investigated the role of CCL3 receptors during severe EV71 infection. The transcriptome analysis was performed on polymorphonuclear neutrophils of patients with mild or critical symptom during EV71 infection. CCR1/3/7 and CXCR1/2/4 were upregulated while CXCR5 was down regulated in critical

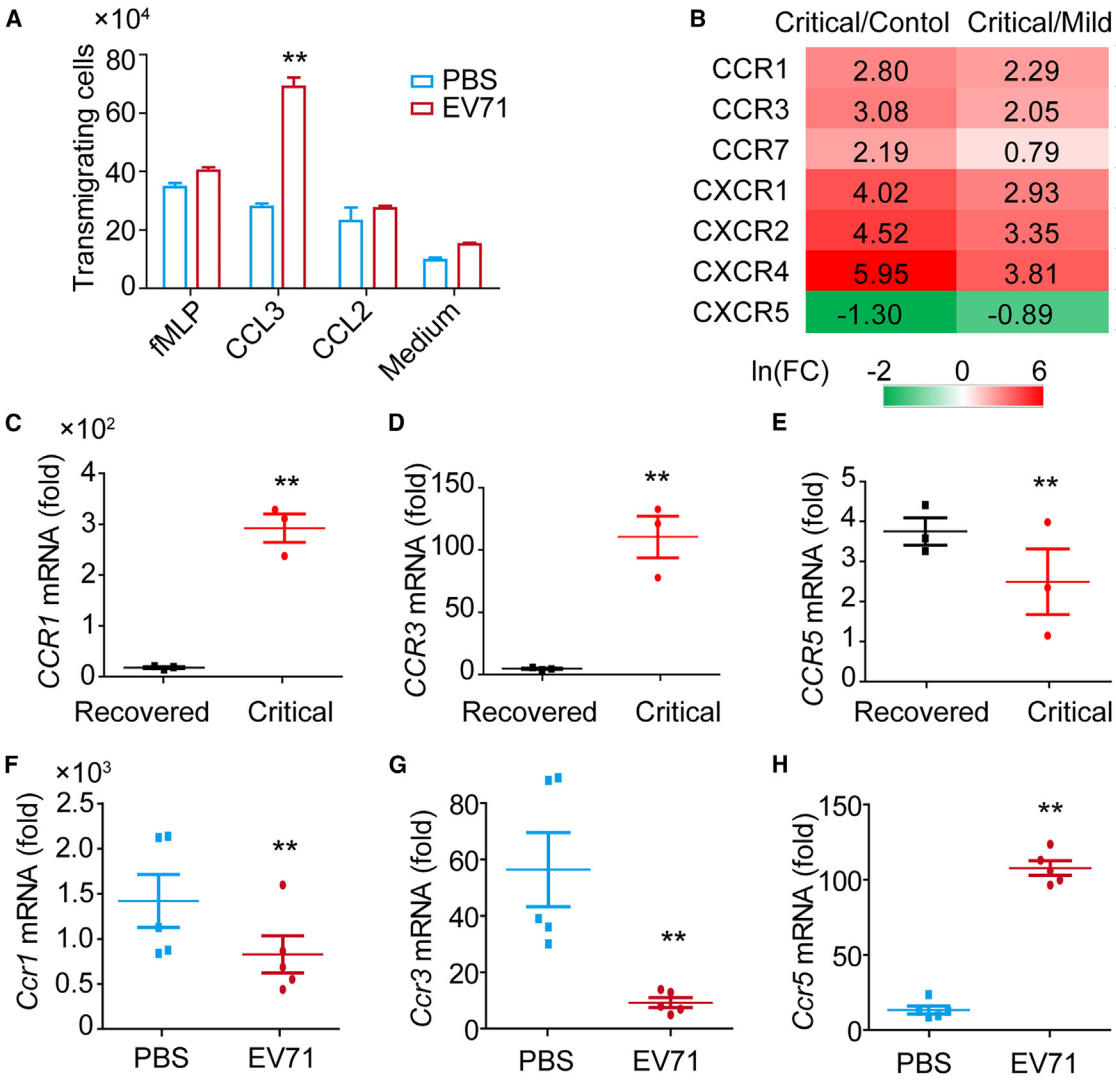

Figure 5. CCL3 recruit neutrophils into the brain through CCR1/3(human) and CCR5(mouse)

(A) Transwell assay for chemotactic ability of neutrophils from EV71-infected mice or PBS-injected mice, in which the CCL3 and CCL2 proteins were placed in the lower chamber and the neutrophils were seeded in the upper chamber and 3 h later the neutrophils that had transversed into the lower chamber were counted. Positive control: fMLP; negative control: RPMI-160 medium.

(B) qPCR analysis chemokine receptors expression in neutrophils from control, mild and critical EV71 infection patients. (C and E) Expression of *CCR1* (C), *CCR3* (D) and *CCR5* (E) on neutrophils in human CSF from patients with EV71 infection during either the acute phase or recovery phase, measured by qRT-PCR.

(F–H) Expression of *Ccr1* (F), *Ccr3* (G) and *Ccr5* (H) on neutrophils in brain tissues from EV71-infected mice or PBS-injected negative control mice, measured by qRT-PCR.

patients compared to control or mild patients (Figure 5B). CCR1/3/5 are the classic receptors of CCL3, we further examined the mRNA expression of CCR1/3/5 in samples of human CSF and mouse brain tissues. CCR1 (Figure 5C) and CCR3 (Figure 5D), but not CCR5 (Figure 5E) in the neutrophils from human CSF was up-regulated during the acute stage of severe immunopathology. While only that of CCR5 was up-regulated in the neutrophils from mouse brain after EV71-infection (Figures 5F–5H). And then we also examined the protein expression of CCR1/3 in samples of CSF from critical and recovered patients and the protein expression of CCR5 in samples of brain tissues from control and EV71 infected mouse (Figures S6A–S6C). CCR1 (Figure S6A) and CCR3 (Figure S6B) in the neutrophils from human CSF was up-regulated during the acute stage of severe immunopathology. While only that of CCR5 was up-regulated in the neutrophils from mouse brain after EV71-infection (Figure S6C). It is suggested that CCL3 may recruit neutrophils to the brain though CCR1/3 in human and CCR5 in mice during EV71 infection, but further validation is required.

Inhibition of CCL3 reduces the neutrophils infiltration in brains and the mortality of EV71 infected mice

Since CCL3-mediated neutrophil recruitment into the brain contributes to the severe immunopathology of EV71 infection, we

further investigated whether blocking CCL3-mediated neutrophil recruitment would alleviate the immunopathology following severe enterovirus 71 infection. Therefore, the severe EV71-infected mice were treated by anti-CCL3 antibodies, which caused decreased CCL3 protein level (Figure 6A) and neutrophils infiltration in brains compared with those of control mice (Figures 6B and 6C). The percent survival (Figure 6D), clinical scores (Figure 6E), and body weight changes (Figure 6F) of anti-CCL3 antibodies-treated mice were sharply improved compared with those of the control mice. In addition, miRNA can bind to the 3′ untranslated region (3′UTR) of CCL3 mRNA in a partially complementary manner, inducing the degradation or translation inhibition of CCL3 mRNA. When specific miRNA binds to CCL3 mRNA, it can lead to decreased stability of CCL3 mRNA or inhibition of translation, resulting in reduced synthesis of CCL3 protein, thereby regulating CCL3. To reveal the post-transcriptional regulatory mechanism of CCL3 in neutrophils after EV71 infection, we performed deep sequencing and bioinformatics analysis on neutrophils before and after EV71 infection in collaboration with technical personnel from Wuhan Life Beauty Biotechnology Co., Ltd. Significant downregulated microRNAs after EV71 infection were analyzed to discover candidate microRNAs targeting CCL3. Through qRT-PCR experiments, 5 candidate microRNAs were selected, including 2 human microRNAs (previously reported Hsa-mir-3653 and unreported Hsa-mir-chr12-2974) and 3 mouse microRNAs (unreported Mmu-mir-chr7-17772, Mmu-mir-chr19-40377, and Mmu-mir-chr18-39664) (Figure S7A). qRT-PCR experiments showed that the 5 microRNAs were expressed in neutrophils of normal brain tissue but significantly decreased after EV71 infection (Figures S7B–S7F), with their sequences listed (Table S4). It was showed that all 5 of these candidate miRNAs markedly inhibited CCL3 expression by luciferase assay analysis, but that their corresponding mutants (scrambled miRNAs) had no inhibitive effects (Figures S7G–S7K). These results provided 5 candidate miRNAs targeting CCL3 for the treatment of EV71 infection. Thus, Mixed-Mmu-mirs were injected i.p. to treat the severe EV71-infected mice. Mixed-Mmu-mirs significantly reduced CCL3 mRNA expression (Figure 6G) and neutrophils infiltration in brains of EV71-infected mice (Figures 6H and 6I). Compared to the 100% rate of death within 1 week among the wild-type (WT) control mice, ∼40% of the miRNAs-treated mice survived through 2 weeks post-infection (Figure 6J). The clinical scores (Figure 6K) and infection-related changes in average body weights (Figure 6L) were in concordance with the survival rate. These results provide 5 candidate miRNAs targeting CCL3 for the treatment of EV71 infection.

DISCUSSION

EV71 is the etiological factor of HFMD and may lead to severe inflammation in brain tissues.[1] The detailed mechanisms underlying EV71 infection, however, remain to be fully clarified, despite the fact that this information is crucial for developing effective treatments for this infection and its life-threatening disease manifestations. Studies of mouse models and human cases of EV71 infection have provided strong cues to suggest that a marked increase of neutrophils count may be an independent risk factor for severe HFMD.[13,14] However, whether and how neutrophils are responsible for progression to the severe disease state remains unclear. This study reveals that the neutrophils play a critical role in establishing and driving the EV71-induced severe immunopathology that can lead to death. Specifically, the chemokine CCL3-recruited neutrophils to the brain mediates this pathogenic process. Moreover, inhibition of CCL3 by anti-CCL3 antibodies or selected miRNAs significantly reduce the neutrophil infiltration in brains and the mortality of EV71-infected mice. These data provide a previously unpublished mechanism of the fatal immunopathology following enterovirus 71 infection.

Though it is known that inflammation critically contributes to neural injury in EV71 infection, there are debates about the roles of innate and adaptive immunity in EV71-induced acute encephalitis. For instance, the reported data about which immune cell types are predominant in infected individuals has ranged from macrophages[15–17] and NK cells[16] to T or B cells.[18,19] In this study, we observed that *Rag1*$^{-/-}$ mice, which lack functional mature T and B cells, have EV71 survival rates and clinical scores that are comparable to those of WT mice, suggesting that the innate immune response is mainly responsible for EV71 infection-induced immunopathology. In accordance with this hypothesis, we also found significantly increased neutrophils and activated monocytes, but without marked alteration in the lymphocyte profile, in peripheral blood and CSF samples from patients with severe EV71 infection as well as infection tissue samples from EV71-infected mice. Collectively, these results support that the innate immune cells might be responsible for the molecular pathogenesis underlying fatality of EV71 infection, with the neutrophils and macrophages acting as the main effectors in this course. The discrepancy in the current literature about the roles of innate and adaptive immunity in EV71-infected cases might due to the sampling time point and/or evaluation of the severity of infection-induced diseases, such as isolated brainstem encephalitis, autonomic nervous system dysregulation, and PE.[12]

Neutrophils are generally considered to play an essential beneficial role in host defense. During bacterial or fungal infections, they are markedly increased in the circulation and tissues, and their decrease (neutropenia, due to genetic defects or chemotherapy) leads to recurrent microbial infections.[20] Moreover, the potent antibacterial and antifungal actions of neutrophils, and the mechanisms of these actions, are well characterized.[21] In contrast, the contribution of neutrophils to antiviral defense is less well studied and has even been contested. Neutrophils are the first and predominant immune cell population recruited to an affected site upon viral infection, in a process triggered by microbial signals and inflammatory mediators such as proinflammatory cytokines (TNF, IL-1, and IL-6), chemokines (CXCL1, CXCL2, and CXCL8), complement component C5a, and leukotriene B4[22]. However, it remains unclear how critical this process is for antiviral immunity in particular. A functional role of neutrophils in antiviral immunity has been proposed for influenza A virus (IAV) infection. Depletion of neutrophils or limitation of neutrophil recruitment was shown to lead to increased lethality of IAV-infected mice.[23,24] A similar protective role of neutrophils has been suggested in other viral infection models, including hepatitis virus, herpes simplex virus (HSV)-1, Marburg and Ebola virus infections.[25–27] Nonetheless, the improper and/or prolonged activation of neutrophils can lead to detrimental

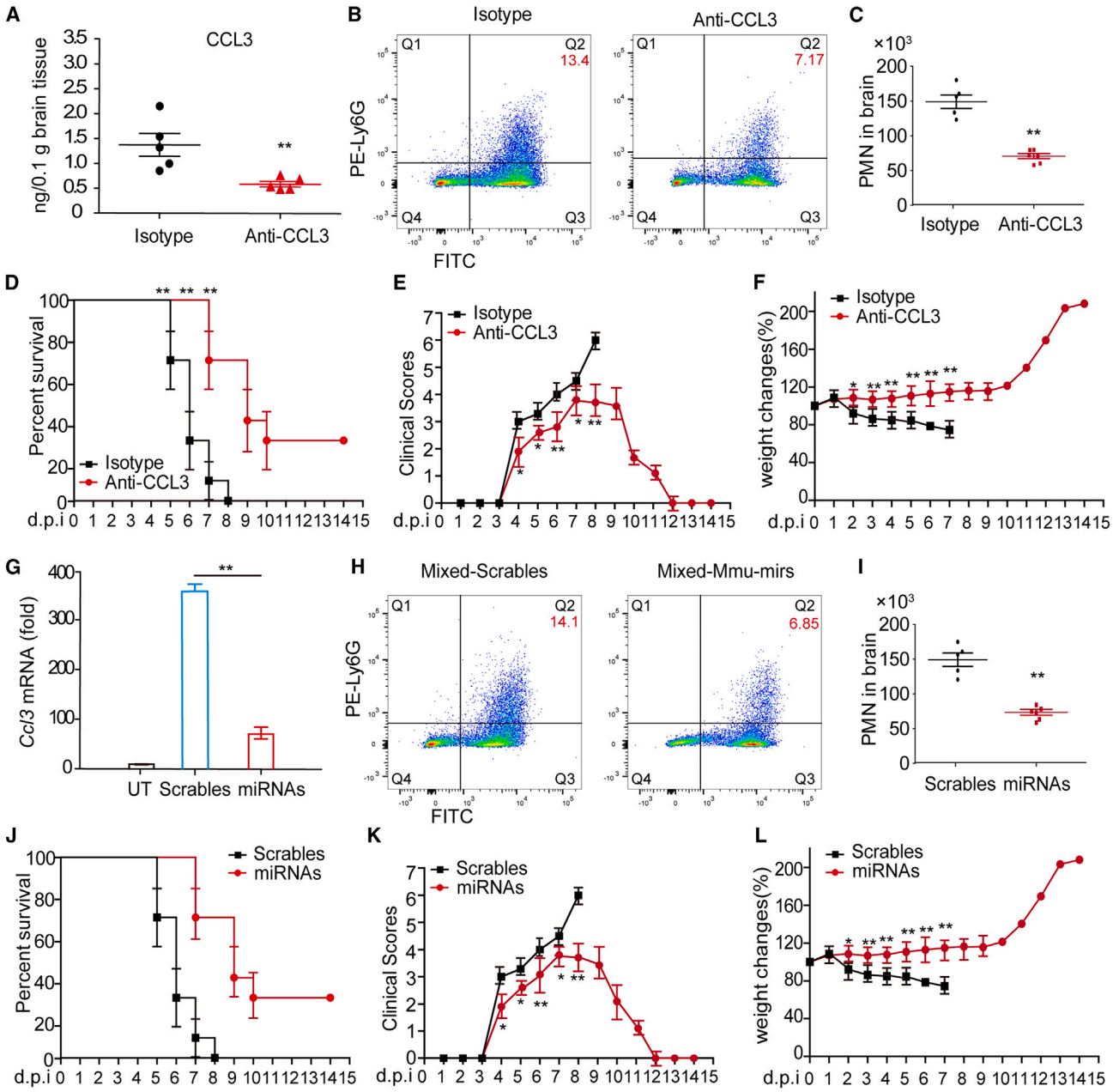

Figure 6. Inhibition of CCL3 reduces the neutrophils infiltration in brains and the mortality of EV71 infected mice

(A–F) EV71-infected mice (100LD_{50}/100 μL/mouse of EV71) were injected i.p. with isotype or anti-CCL3 antibody (100 μg/100 μL/mouse).

(A) ELISA analysis the CCL3 expression in mice brain tissues.

(C and B) Leukocytes were isolated from brain tissues of EV71-infected mice by use of the Ficoll Reagent on day 6 dpi and stained with anti-CD45-FITC and anti-Ly6G-PE. The percentages of neutrophils (CD45+Ly6G+) in total leukocytes were detected by FCM assay (C) and the corresponding statistical analyses are shown (B).

(D–F) The mortality (D), body weight (E) and clinical scores (F) of mice were monitored and recorded daily after infection.

(G–L) EV71-infected mice (100LD_{50}/100 μL/mouse of EV71) were injected i.p. with Mixed-scrables or Mixed-mmu-mirs (90 μg/g body weight), (G) qPCR analysis the *Ccl3* mRNA expression in mice brain tissues.

(H and I) Leukocytes were isolated from brain tissues of EV71-infected mice by use of the Ficol Reagent on day 6 dpi and stained with anti-CD45-FITC and anti-Ly6G-PE. The percentages of neutrophils ($CD45^+Ly6G^+$) in total leukocytes were detected by FCM assay (H) and the corresponding statistical analyses are shown (I).

(J–L) The mortality (J), body weight (K) and clinical scores (L) of mice (G) were monitored and recorded daily after infection.

effects on host cells and tissues, manifesting as severe disease as has been shown in viral infection mouse models such as IAV, HSV, murine cytomegalovirus and human rhinovirus (detailed review in ref.[28]).

Although the beneficial or detrimental roles of neutrophils often correlated with viral load in experimental animals, we found that depletion of neutrophils markedly alleviated the EV71-induced disease but it did not affect the viral load in different tissues, in accordance with the observation from Sakai Sand colleagues under the conditions of influenza infection.[29] This finding is also in accordance with the recent results from an analysis of a large amount of transcriptomic data using a systemic biology approach, in which influenza lethality was found to not be associated with the pathogen's cytopathic action but rather with the inflammatory response orchestrated by the host.[30] Specifically, it was demonstrated that lethal influenza infection in mice correlated better with excessive neutrophil activation than with the viral load and was linked to the presence of a proinflammatory transcriptional signature comprising TNF, IL-1, IL-6, acute phase response genes and the NF-κB, JAK-STAT, and MAPK signaling cascades.[30]

Indeed, we found that although amounts of cytokines and chemokines were elevated in the sera of patients and mice post-infection, only levels of the chemokines CCL-2, CCL-3, CCL-4 and CCL-5 and of the cytokines IL-6 and G-CSF were significantly increased in CSF of infected patients, among which CCL-3 and CCL-2 were the most robustly increased chemokines. Neutrophil recruitment to inflamed local sites is mediated by several factors, including the chemokines CXCL1, CXCL2 and CXCL8[22] as shown in animal models of pathogenic infection (mice) or sterile injury (zebrafish).[28,31,32] However, the levels of these chemokines were not altered significantly in our mouse model of EV71 infection. CCL-2 and CCL-3 can contribute to migration of monocytes and macrophages,[33] and CCL-3 can mediate that of neutrophils as well.[34–36] In our study of EV71 infection, CCL3 (compared to CCL-2) appeared to be the main chemokine mediating neutrophil migration to the brain tissue. Anti-CCL-3-treated and CCL-3 KO mice showed a sharp decrease in neutrophil migration to brain tissue, unlike the anti-CCL-2-treated and CCL-2 KO mice that showed no effect on neutrophil migration as compared to the WT controls.

The human cases of acute phase severe EV71 infection in our study also showed elevated expression of CCR1 and CCR3 genes in neutrophils isolated from CSF. In contrast, the EV71-infected mice showed elevated CCR5 gene expression in neutrophils isolated from brain tissues. All three of these CCRs have been reported as candidate receptors for CCL3, and all three are expressed on neutrophils.[33] Thus, humans and mice may use distinctive chemotaxis modes for neutrophil transmigration during EV71 infection. The CCL3-CCR1/CCR3/CCR5 may be pivotal for neutrophil migration and the fatal pathology of EV71 infection because CCL3 neutralization or KO led to enhanced survival rate of infected mice in our study. Accordingly, inhibition of neutrophil migration into brain tissues by targeting CCL3 significantly decreased inflammation in brain tissue of EV71-infected mice, which occurred, at least partly, through a decrease in the oxidative burst of neutrophils, one of the main effector mechanisms of this immune cell type.[22]

CCL3 expression might be regulated at the post-transcriptional level, such as by means of miRNAs, the short, conserved, non-coding RNA molecules that modulate mRNA translation and/or degradation.[37] Recent investigations by others have suggested that distinct miRNAs play roles in the maintenance of immune homeostasis and the induction of immune defense, and are involved in protection against bacterial infections.[38,39] Recently, Dorhoi et al.[40] reported that miR-223 controls recruitment of myeloid cells to lung during tuberculosis, leading to neutrophil-driven lethal inflammation by directly targeting CXCL2, CCL3 and IL-6 in the myeloid cells. EV71 infection may lead to the regulation of miRNA synthesis and degradation processes within the cell, resulting in changes in miRNA levels. In the present study, we identified 5 miRNAs targeting the CCL3 gene. All these miRNAs were significantly down-regulated during EV71 infection, and the *in vitro* assays confirmed their remarkable inhibitive ability on CCL3 expression. Thus, the study presented herein provided new candidate miRNAs for the regulation of CCL3 expression during EV71 infection, the clinical utility of which needs to be verified in future studies. EV71 may directly interact with the host cell's miRNA processing machinery. EV71 could potentially alter the expression or activity of miRNA processing enzymes, such as Drosha or Dicer, leading to global changes in miRNA levels within the cell. Additionally, EV71 may also induce specific cellular signaling pathways that regulate the expression of certain miRNAs involved in immune response or antiviral defense mechanisms. Further research is needed to fully understand the precise mechanisms by which EV71 infection impacts miRNA levels in host cells.

In conclusion, this study discovered that the recruitment of CCL3-mediated neutrophils to brain is critical for the fatal immunopathology of EV71 infection, suggesting that CCL3 is a potential intervening therapeutic target, although other innate and adaptive immune cells may also exert protective or detrimental effects during EV71 infection and may complicate this proposed approach or serve as targets themselves to enhance the approach. Antagonists or inhibitors of the human CCL3 cognate receptors CCR1 and CCR3 may be in clinical trials for treatment of rheumatoid arthritis, multiple sclerosis, psoriasis, eczema, Alzheimer's disease, rhinitis, conjunctivitis, asthma, and allergic rhinitis, based upon their ability to block the recruitment of T cells, monocytes, eosinophils, basophils and mast cells.[41–43] It is possible, then, that these antagonists may be effective for the treatment of EV71 infection as well. In addition, miRNAs might also be used for treating fatal EV71 infection, particularly relying on their potential to down-regulate the detrimental roles of neutrophils exerted on host tissues (bystander injury). Therefore, this study not only provides concrete evidence for the roles and the underlying mechanisms of CCL3 in mediating critical pathological effects of neutrophils in EV71 infection but also provides potential therapeutic targets for EV71 infection.

Limitations of the study

In previous studies, CCR1, CCR3, and CCR5 have been confirmed as receptors for CCL3. In this study, we examined the expression of these receptors at both the mRNA and protein levels in severe EV71 patients and mice. Our findings suggest

that CCR1 and CCR3 may play an important role in CCL3-mediated neutrophil accumulation in the brains of patients. However, further experiments are necessary to individually knock down or block these receptors in future work.

RESOURCE AVAILABILITY

Lead contact

Further information and any requests should be directed to and will be fulfilled by the lead contact, Min Li (luckylixiaomi@163.com).

Materials availability

This study did not generate new unique reagents.

Data and code availability

- The datasets generated and analyzed related to this paper are available from the lead contact on reasonable request.
- This paper does not report original code.
- Any additional information required to reanalyze the data reported in this paper is available from the lead contact upon request.

ACKNOWLEDGMENTS

We thank the patients, their families, and all healthy volunteers for their participation in the study. Funding: This work was supported by grants from the National Natural Science Foundation of China (82102369, and 32200711), the National Key Research and Development Plan of China (2021YFC2300200), the Project of State Key Laboratory (SKLPB2224).

AUTHOR CONTRIBUTIONS

W.X.Y. and M.L. conducted most of the experiments and analyzed the data. Y.L.S. and Y.W.W. helped with mouse experiments. W.Z.L. and G.L.L. provided the clinical samples. Y.W. and X.L.H. helped with molecular cloning. W.W.G., J.T., J.X.S. and K.J.Z. provided technical support. Y.T. and X.Y. performed bioinformatics analyses. B.G., L.S., G.Y.Z. and M.L. designed the experiments, supervised the study and wrote the manuscript.

DECLARATION OF INTERESTS

The authors declare no competing interests.

STAR★METHODS

Detailed methods are provided in the online version of this paper and include the following:

- KEY RESOURCES TABLE
- EXPERIMENTAL MODEL AND STUDY PARTICIPANT DETAILS
  - Ethics statement
  - Study participants and sample collection
- METHOD DETAILS
  - Animal experiment
  - Leukocyte counting
  - Flow cytometric (FCM) assay
  - Cytokine and chemokine measurement
  - Histology and immunohistochemistry
  - Chemotaxis assay
  - qRT-PCR
  - Western blotting
  - Deep sequencing and data analysis
  - 3′-UTR cloning and luciferase reporter assay
- QUANTIFICATION AND STATISTICAL ANALYSIS

SUPPLEMENTAL INFORMATION

Supplemental information can be found online at https://doi.org/10.1016/j.isci.2024.111388.

Received: January 5, 2024
Revised: April 27, 2024
Accepted: November 11, 2024
Published: November 15, 2024

REFERENCES

1. Solomon, T., Lewthwaite, P., Perera, D., Cardosa, M.J., McMinn, P., and Ooi, M.H. (2010). Virology, epidemiology, pathogenesis, and control of enterovirus 71. Lancet Infect. Dis. *10*, 778–790.
2. Ooi, M.H., Wong, S.C., Lewthwaite, P., Cardosa, M.J., and Solomon, T. (2010). Clinical features, diagnosis, and management of enterovirus 71. Lancet Neurol. *9*, 1097–1105.
3. Wang, S.M. (2016). Milrinone in Enterovirus 71 Brain Stem Encephalitis. Front. Pharmacol. *7*, 82.
4. Shieh, W.J., Jung, S.M., Hsueh, C., Kuo, T.T., Mounts, A., Parashar, U., Yang, C.F., Guarner, J., Ksiazek, T.G., Dawson, J., et al. (2001). Pathologic studies of fatal cases in outbreak of hand, foot, and mouth disease, Taiwan. Emerg. Infect. Dis. *7*, 146–148.
5. Yang, Y., Wang, H., Gong, E., Du, J., Zhao, X., McNutt, M.A., Wang, S., Zhong, Y., Gao, Z., and Zheng, J. (2009). Neuropathology in 2 cases of fatal enterovirus type 71 infection from a recent epidemic in the People's Republic of China: a histopathologic, immunohistochemical, and reverse transcription polymerase chain reaction study. Hum. Pathol. *40*, 1288–1295.
6. Marcus, C.L. (2001). Nasal steroids as treatment for obstructive sleep apnea: Don't throw away the scalpel yet. J. Pediatr. *138*, 795–797.
7. Huang, C.C., Liu, C.C., Chang, Y.C., Chen, C.Y., Wang, S.T., and Yeh, T.F. (1999). Neurologic complications in children with enterovirus 71 infection. N. Engl. J. Med. *341*, 936–942.
8. Weng, K.F., Chen, L.L., Huang, P.N., and Shih, S.R. (2010). Neural pathogenesis of enterovirus 71 infection. Microb. Infect. *12*, 505–510.
9. LaFrance-Corey, R.G., and Howe, C.L. (2011). Isolation of brain-infiltrating leukocytes. J. Vis. Exp. 2747.
10. Wang, S.M., Lei, H.Y., Yu, C.K., Wang, J.R., Su, I.J., and Liu, C.C. (2008). Acute chemokine response in the blood and cerebrospinal fluid of children with enterovirus 71-associated brainstem encephalitis. J. Infect. Dis. *198*, 1002–1006.
11. Lin, T.Y., Chang, L.Y., Huang, Y.C., Hsu, K.H., Chiu, C.H., and Yang, K.D. (2002). Different proinflammatory reactions in fatal and non-fatal enterovirus 71 infections: implications for early recognition and therapy. Acta Paediatr. *91*, 632–635.
12. Wang, S.M., Lei, H.Y., Huang, K.J., Wu, J.M., Wang, J.R., Yu, C.K., Su, I.J., and Liu, C.C. (2003). Pathogenesis of enterovirus 71 brainstem encephalitis in pediatric patients: roles of cytokines and cellular immune activation in patients with pulmonary edema. J. Infect. Dis. *188*, 564–570.
13. Liao, C.C., Liou, A.T., Chang, Y.S., Wu, S.Y., Chang, C.S., Lee, C.K., Kung, J.T., Tu, P.H., Yu, Y.Y., Lin, C.Y., et al. (2014). Immunodeficient mouse models with different disease profiles by *in vivo* infection with the same clinical isolate of enterovirus 71. J. Virol. *88*, 12485–12499.
14. Chew, S.P., Chong, S.L., Barbier, S., Matthew, A., Lee, J.H., and Chan, Y.H. (2015). Risk factors for severe hand foot mouth disease in Singapore: a case control study. BMC Infect. Dis. *15*, 486.
15. Chen, M.F., Weng, K.F., Huang, S.Y., Liu, Y.C., Tseng, S.N., Ojcius, D.M., and Shih, S.R. (2016). Pretreatment with a heat-killed probiotic modulates monocyte chemoattractant protein-1 and reduces the pathogenicity of influenza and enterovirus 71 infections. Mucosal Immunol. *10*, 215–227.
16. Zhu, K., Yang, J., Luo, K., Yang, C., Zhang, N., Xu, R., Chen, J., Jin, M., Xu, B., Guo, N., et al. (2015). TLR3 signaling in macrophages is indispensable

for the protective immunity of invariant natural killer T cells against enterovirus 71 infection. PLoS Pathog. *11*, e1004613.

17. Liu, J., Li, X., Fan, X., Ma, C., Qin, C., and Zhang, L. (2013). Adoptive transfer of macrophages from adult mice reduces mortality in mice infected with human enterovirus 71. Arch. Virol. *158*, 387–397.
18. Xie, J., Jiao, Y., Qiu, Z., Li, Q., and Li, T. (2010). Significant elevation of B cells at the acute stage in enterovirus 71-infected children with central nervous system involvement. Scand. J. Infect. Dis. *42*, 931–935.
19. Lin, Y.W., Chang, K.C., Kao, C.M., Chang, S.P., Tung, Y.Y., and Chen, S.H. (2009). Lymphocyte and antibody responses reduce enterovirus 71 lethality in mice by decreasing tissue viral loads. J. Virol. *83*, 6477–6483.
20. Lekstrom-Himes, J.A., and Gallin, J.I. (2000). Immunodeficiency diseases caused by defects in phagocytes. N. Engl. J. Med. *343*, 1703–1714.
21. Amulic, B., Cazalet, C., Hayes, G.L., Metzler, K.D., and Zychlinsky, A. (2012). Neutrophil function: from mechanisms to disease. Annu. Rev. Immunol. *30*, 459–489.
22. Mayadas, T.N., Cullere, X., and Lowell, C.A. (2014). The multifaceted functions of neutrophils. Annu. Rev. Pathol. *9*, 181–218.
23. Tate, M.D., Deng, Y.M., Jones, J.E., Anderson, G.P., Brooks, A.G., and Reading, P.C. (2009). Neutrophils ameliorate lung injury and the development of severe disease during influenza infection. J. Immunol. *183*, 7441–7450.
24. Allen, I.C., Scull, M.A., Moore, C.B., Holl, E.K., McElvania-TeKippe, E., Taxman, D.J., Guthrie, E.H., Pickles, R.J., and Ting, J.P.Y. (2009). The NLRP3 inflammasome mediates *in vivo* innate immunity to influenza A virus through recognition of viral RNA. Immunity *30*, 556–565.
25. Zhou, J., Stohlman, S.A., Hinton, D.R., and Marten, N.W. (2003). Neutrophils promote mononuclear cell infiltration during viral-induced encephalitis. J. Immunol. *170*, 3331–3336.
26. Tumpey, T.M., Chen, S.H., Oakes, J.E., and Lausch, R.N. (1996). Neutrophil-mediated suppression of virus replication after herpes simplex virus type 1 infection of the murine cornea. J. Virol. *70*, 898–904.
27. Mohamadzadeh, M., Coberley, S.S., Olinger, G.G., Kalina, W.V., Ruthel, G., Fuller, C.L., Swenson, D.L., Pratt, W.D., Kuhns, D.B., and Schmaljohn, A.L. (2006). Activation of triggering receptor expressed on myeloid cells-1 on human neutrophils by marburg and ebola viruses. J. Virol. *80*, 7235–7244.
28. Galani, I.E., and Andreakos, E. (2015). Neutrophils in viral infections: Current concepts and caveats. J. Leukoc. Biol. *98*, 557–564.
29. Sakai, S., Kawamata, H., Mantani, N., Kogure, T., Shimada, Y., Terasawa, K., Sakai, T., Imanishi, N., and Ochiai, H. (2000). Therapeutic effect of anti-macrophage inflammatory protein 2 antibody on influenza virus-induced pneumonia in mice. J. Virol. *74*, 2472–2476.
30. Brandes, M., Klauschen, F., Kuchen, S., and Germain, R.N. (2013). A systems analysis identifies a feedforward inflammatory circuit leading to lethal influenza infection. Cell *154*, 197–212.
31. Sarris, M., Masson, J.B., Maurin, D., Van der Aa, L.M., Boudinot, P., Lortat-Jacob, H., and Herbomel, P. (2012). Inflammatory chemokines direct and restrict leukocyte migration within live tissues as glycan-bound gradients. Curr. Biol. *22*, 2375–2382.
32. McDonald, B., Pittman, K., Menezes, G.B., Hirota, S.A., Slaba, I., Waterhouse, C.C.M., Beck, P.L., Muruve, D.A., and Kubes, P. (2010). Intravascular danger signals guide neutrophils to sites of sterile inflammation. Science *330*, 362–366.
33. Griffith, J.W., Sokol, C.L., and Luster, A.D. (2014). Chemokines and chemokine receptors: positioning cells for host defense and immunity. Annu. Rev. Immunol. *32*, 659–702.
34. Ottonello, L., Montecucco, F., Bertolotto, M., Arduino, N., Mancini, M., Corcione, A., Pistoia, V., and Dallegri, F. (2005). CCL3 (MIP-1alpha) induces *in vitro* migration of GM-CSF-primed human neutrophils via CCR5-dependent activation of ERK 1/2. Cell. Signal. *17*, 355–363.
35. Ramos, C.D.L., Canetti, C., Souto, J.T., Silva, J.S., Hogaboam, C.M., Ferreira, S.H., and Cunha, F.Q. (2005). MIP-1alpha[CCL3] acting on the CCR1 receptor mediates neutrophil migration in immune inflammation via sequential release of TNF-alpha and LTB4. J. Leukoc. Biol. *78*, 167–177.
36. Cook, D.N., Beck, M.A., Coffman, T.M., Kirby, S.L., Sheridan, J.F., Pragnell, I.B., and Smithies, O. (1995). Requirement of MIP-1 alpha for an inflammatory response to viral infection. Science *269*, 1583–1585.
37. Krol, J., Loedige, I., and Filipowicz, W. (2010). The widespread regulation of microRNA biogenesis, function and decay. Nat. Rev. Genet. *11*, 597–610.
38. O'Connell, R.M., Rao, D.S., Chaudhuri, A.A., and Baltimore, D. (2010). Physiological and pathological roles for microRNAs in the immune system. Nat. Rev. Immunol. *10*, 111–122.
39. Eulalio, A., Schulte, L., and Vogel, J. (2012). The mammalian microRNA response to bacterial infections. RNA Biol. *9*, 742–750.
40. Dorhoi, A., Iannaccone, M., Farinacci, M., Faé, K.C., Schreiber, J., Moura-Alves, P., Nouailles, G., Mollenkopf, H.J., Oberbeck-Müller, D., Jörg, S., et al. (2013). MicroRNA-223 controls susceptibility to tuberculosis by regulating lung neutrophil recruitment. J. Clin. Invest. *123*, 4836–4848.
41. Szekanecz, Z., and Koch, A.E. (2004). Therapeutic inhibition of leukocyte recruitment in inflammatory diseases. Curr. Opin. Pharmacol. *4*, 423–428.
42. Godessart, N. (2005). Chemokine receptors: attractive targets for drug discovery. Ann. N. Y. Acad. Sci. *1051*, 647–657.
43. Charo, I.F., and Ransohoff, R.M. (2006). The many roles of chemokines and chemokine receptors in inflammation. N. Engl. J. Med. *354*, 610–621.
44. Mao, Q., Wang, Y., Gao, R., Shao, J., Yao, X., Lang, S., Wang, C., Mao, P., Liang, Z., and Wang, J. (2012). A neonatal mouse model of coxsackievirus A16 for vaccine evaluation. J. Virol. *86*, 11967–11976.
45. Kimmey, J.M., Huynh, J.P., Weiss, L.A., Park, S., Kambal, A., Debnath, J., Virgin, H.W., and Stallings, C.L. (2015). Unique role for ATG5 in neutrophil-mediated immunopathology during M. tuberculosis infection. Nature *528*, 565–569.
46. McKenzie, C.G.J., Kim, M., Singh, T.K., Milev, Y., Freedman, J., and Semple, J.W. (2014). Peripheral blood monocyte-derived chemokine blockade prevents murine transfusion-related acute lung injury (TRALI). Blood *123*, 3496–3503.
47. Goser, S., Ottl, R., Brodner, A., Dengler, T.J., Torzewski, J., Egashira, K., Rose, N.R., Katus, H.A., and Kaya, Z. (2005). Critical role for monocyte chemoattractant protein-1 and macrophage inflammatory protein-1alpha in induction of experimental autoimmune myocarditis and effective anti-monocyte chemoattractant protein-1 gene therapy. Circulation *112*, 3400–3407.

STAR★METHODS

KEY RESOURCES TABLE

REAGENT or RESOURCE	SOURCE	IDENTIFIER
Antibodies		
anti-Ly6G MAb, 1A8	BioLegend	Cat#orb1672083
anti-CCL3 MAb	R&D Systems Inc.	Cat# MAB66252
anti-CCL2 MAb	R&D Systems Inc.	Cat# #123616
anti-CD19	BD Pharmingen of BD Biosciences	Cat# #555412
anti-CD3	BD Pharmingen of BD Biosciences	Cat# #570821
anti-CD4	BD Pharmingen of BD Biosciences	Cat# #556615
anti-CD8	BD Pharmingen of BD Biosciences	Cat# #555367
Bacterial and virus strains		
EV71 strain TS	Zhao,Z.P et al.	GenBank No. JQ708210.1
Biological samples		
the peripheral blood and the CSF of EV71-infected patients	Ditan Hospital and Fengtai Maternal & Child Health Care Hospital	licensing number: Jing You Ke Lun[2018]045
Chemicals, peptides, and recombinant proteins		
N-formyl-methionyl-leucyl-phenylalanine	Sigma-Aldrich	Cat#F3506
Critical commercial assays		
TRIzol Reagent	Invitrogen	Cat#15596018CN
Neutrophil Separation Kit	Hao Yang Biological Manufacture Co., Ltd	Cat#LZS11131
murine CCL3 ELISA kit	Boster Biological Engineering Co.,Ltd	EK0449
murine CCL2 ELISA kit	Boster Biological Engineering Co.,Ltd	EK0568
human CCL3 ELISA kit	Boster Biological Engineering Co.,Ltd	EK0448
human CCL2 ELISA kit	Boster Biological Engineering Co.,Ltd	EK0441
Bio-Plex Mouse Cytokine Group I 23-Plex	Bio-Rad	M60009RDPD
Bio-Plex Human Cytokine Group I 27-Plex	Bio-Rad	M500KCAF0Y
mirVana miRNA isolation kit	ThermoFisher Scientific	AM1561
Deposited data		
CCL-3 in human	NCBI	GenBank No. NM_002983.2
CCL-3 in C57BL/6 mouse	NCBI	GenBank No. NM_011337.2
Hsa-mir-3653	https://www.mirbase.org/	Accession:MI0016053
Hsa-mir-Chr12-2974	NCBI	ID number:2886035
Mmu-mir-chr7-17772	NCBI	ID number:2886035
Mmu-mir-chr19-40377	NCBI	ID number:2886035
Mmu-mir-chr18-39664	NCBI	ID number:2886035
Experimental models: Cell lines		
293T cells	ATCC	CL-0005
Experimental models: Organisms/strains		
CCL3 knock-out (KO) mice	The Jackson Laboratory	Stock No. 002687
CCL2 knock-out (KO) mice	The Jackson Laboratory	Stock No. 004434
Oligonucleotides		
qRT-PCR primers Table S2	This paper	N/A
Software and algorithms		
GraphPad Prism 8.0 program	GraphPad Software, Inc.	https://www.graphpad.com/scientific-software/prism
CellQuestTM analysis software	BD Biosciences	https://www.bdbiosciences.com/

EXPERIMENTAL MODEL AND STUDY PARTICIPANT DETAILS

Ethics statement

All the animal experiments performed in this study were approved and licensed by the Medical Ethics Branch Committee of the Supervisory Committee of Science and Technology of the Academy of Military Medical Science (AMMS), Beijing, China (Licensing number: IACUC of AMMS-2009-02). Use of human samples for the study was approved and licensed by the Institutional Ethical Committees of You'an Hospital Capital Medical University, Beijing, China (licensing number: Jing You Ke Lun[2018]045). All adult subjects provided informed written consent; for child participants informed written consent was provided by the parent/guardian of the child.

Study participants and sample collection

EV71 strain TS (GenBank No. JQ708210.1) was isolated by Zhao,Z.P et al.

CCL3 (Stock No. 002687), CCL2 (Stock No. 004434) and Rag-1 (Stock No. 002216) knock-out (KO) mice (femal, 14-days-old), which were all C57BL/6 background, were purchased from The Jackson Laboratory (Bar Harbor, ME, USA). Wild-type (WT) C57BL/6 mice(femal, 14-days-old) were bred at the animal facility of the AMMS Laboratory Animal Center, and used as sex- and age-matched controls for the various KO strains. Mice were housed and treated in accordance with academic guidelines.

Blood samples from a total of 70 children (age range 6 months to 5 years, male:female ratio 1.12:1) were analysed in this study. Of these children, 50 had been diagnosed with EV71 infection and 20 were as healthy controls. Every individual's age, sex and EV71 infection diagnosis is provided in Table S1. Diagnosis of EV71 monoinfection was established by quantitative real-time reverse transcription-PCR (qRT-PCR) of one or more throat swabs, stool specimens, blood, cerebrospinal fluid (CSF) were collected from each patient on the day of admission. For the severe (inpatient) cases, samples were also collected on the day of discharge. Control samples were obtained from 20 age-matched children who presented for routine health examination and showed no contagious or commonly encountered diseases (Table S1). Every sample was handled according to HFMD Prevention & Control Guidelines (2008) and immediately assayed or stored in aliquots of 0.1 mL at -80^{o}C until assayed.

METHOD DETAILS

Animal experiment

At 14-days-old, the mice were infected i.p. with 100 LD_{50} of the EV71 strain TS (GenBank No. JQ708210.1; 3200 PFU in 100 μL), denoted as day 0 (time of viral challenge).[44] For depletion of neutrophils, 100 μg/mouse of purified neutralizing monoclonal rat anti-mouse Ly6G IgG antibody (anti-Ly6G MAb, 1A8; BioLegend, San Diego, USA) was injected i.p. at 1, 3 and 5 days post-infection (dpi)[40,45]; suckling mice from the control group were injected with 100 μg of purified rat IgG (isotype control) (BioLegend). For depletion of macrophages, 250 μg/mouse of gadolinium (III) chloride hexahydrate (in 100 μL PBS; Sigma-Aldrich, St. Louis, MO, USA) was injected i.p. at 1, 3 and 5 dpi[46]; suckling mice from the control group were injected with 100 μL of PBS. For knocking-down CCL3, 50 μg/mouse of purified neutralizing anti-CCL3 MAb (R&D Systems Inc., Minneapolis, MN, USA) was injected i.p. at 1, 3 and 5 dpi; suckling mice from the control group were injected with 50 μg of purified isotype control (R&D Systems).[40] For knocking-down CCL2, 100 μg/mouse of purified neutralizing anti-CCL2 MAb (R&D Systems) was injected i.p. at 1, 3 and 5 dpi[47]; suckling mice from the control group were injected with 100 μg of purified isotype control (R&D Systems). All suckling mice were weighed and monitored daily upon infection; onset and type of clinical symptoms were recorded, and mortality (up to 14 dpi) was taken as the experimental endpoint. The following scoring system was used to classify clinical symptoms: 0, healthy; 1, ruffled hair and hunchbacked; 2, reduced mobility; 3, reduced body weight and limb weakness; 4, limb paralysis; 5, moribund; 6, death.

Leukocyte counting

Analysis of CSF from patients with EV71 infection and HFMD included total nucleated cell count and cell typing (Wright-Giemsa stain; Leagene Biotech. Co, Ltd, Beijing, China). Cell types were expressed as percentage of the total nucleated cell count from the sample.

Flow cytometric (FCM) assay

Mouse brain infiltrating leukocytes (BILs) were isolated from EV71-infected or sham-infected mice and immunophenotyped.[9] The isolated BILs were stained with fluorescent-labeled antibodies against mouse surface cell markers (unless otherwise specified, BD Pharmingen of BD Biosciences, San Jose, CA): FITC-anti-CD19 for B cells; FITC-anti-CD3, Percp-anti-CD4 and PE-anti-CD8 for T cells; FITC-anti-CD45 for leukocytes; PE-anti-NK1.1 for NK cells; PE-anti-CD11c for dendritic cells; PE-anti-Siglec-F for eosinophils; PE-anti-FcεRIα (BioLegend) for basophils; PE-anti-Ly6G for neutrophils; PE-anti-F4/80 (eBioscience, San Diego, CA); APC-anti-Gr-1/(Ly6G and Ly6C) for monocytes. Each sample was also stained with isotype controls for each type of cell. The cell type assessment was carried out by FACSCalibur™ flow cytometer equipped with CellQuest™ analysis software (BD Biosciences). Each cell type count was expressed as percentage of the total BIL cell count.

Cytokine and chemokine measurement

Mouse plasma, supernatants of brain tissue homogenates or cultured cell samples were assayed using murine CCL3 and CCL2 specific ELISA kits (Boster Biological Engineering Co., Ltd, Wuhan, China) and the Bio-Plex Mouse Cytokine Group I 23-Plex (Bio-Rad,

Hercules, USA). Human plasma and CSF samples were assayed using human CCL3 and CCL2 specific ELISA kits (Boster Biological Engineering Co., Ltd) and the Bio-Plex Human Cytokine Group I 27-Plex (Bio-Rad). The array analyses were performed using the Bio-Plex® 200 Protein Array System (Bio-Rad).

Histology and immunohistochemistry

Mouse brain tissues were fixed in 10% buffered formalin, embedded in paraffin, sectioned (4 mm thick) and processed for histologic analysis by staining with hematoxylin and eosin (HE) and for immunohistochemical analysis by staining with the following antibodies: FITC-labeled rat anti-mouse Ly-6G monoclonal antibody (Ly6G-FITC) (Miltenyi Biotec, Cologne, Germany) to detect neutrophils; F4/80-FITC (eBioscience) to detect macrophages; anti-CCL3 (Yaji Biological Technology Co., Ltd, Shanghai, China) to detect T cells. All sections were counterstained with DAPI (Beyotime Institute of Biotechnology, Jiangsu, China) and imaged using a BX61 fluorescence microscope (Olympus, Tokyo, Japan). The semiquantitative assessment were performed as reported previously and described briefly as the following (Haagmans et al., 2004). Degree of inflammatory cells infiltration, we scored 0 when no inflammatory cell infiltration, scored1 when occasional infiltration of single inflammatory cell is visible, and scored 2 when focal infiltration of inflammatory cells is visible.

Chemotaxis assay

Mouse neutrophils were isolated from bone marrow using the Neutrophil Separation Kit by Hao Yang Biological Manufacture Co., Ltd (Tianjin, China). Neutrophil chemotaxis toward CCL3 or CCL2 was assayed using the QCM^{TM} Chemotaxis 3-μm 96-well Cell Migration Assay Kit by Chemicon International, Inc. (Temecula, CA). Briefly, EV71- or mock-treated neutrophils were allowed to migrate toward CCL3 or CCL2 for 3 hours in the presence or absence of recombinant mouse CCL3 (15 ng/mL) or CCL2 (15 ng/mL) (R&D Systems). RPMI-1640 culture medium (Invitrogen/Gibco, Carlsbad, CA) and N-formyl-methionyl-leucyl-phenylalanine (fMLP; 30 μM) (Sigma-Aldrich) served as the negative and positive controls respectively. The migratory cell count was quantified manually using a hemocytometer.

qRT-PCR

EV71 VP1 (to determine EV71 copy number), cellular RNA and microRNA were measured by qRT-PCR. RNA was extracted from cells or tissues using the TRIzol Reagent (Invitrogen). First-strand cDNA for EV71 VP1 or cellular RNA was first synthesized from the DNA-free RNA by using the SuperScript VILO MasterMix (Invitrogen) and then subjected to real-time PCR quantification using a LightCycler 96 (Roche Diagnostics, Mannheim, Germany); glyceraldehyde 3-phosphate dehydrogenase (GAPDH) was amplified as the control. The qRT-PCR analysis of microRNAs was performed with the miDETECT A Track^{TM} miRNA qRT-PCR Starter Kit (RiboBio Co., Ltd, Guangzhou, China); U6 snRNA was amplified as the control. The comparative threshold cycle (CT) method was used to calculate relative amounts of cellular RNA or miRNA and the copy number of EV71 VP1; for the latter, the calculated CT value was transformed to viral RNA copies per mg tissue with respect to the value obtained from amplification of the EV71 VP1 reference gene in the pMD18T plasmid (Takara, Tokyo, Japan). All sequences of qRT-PCR primers used in this study are shown in Table S2.

Western blotting

To detect the CCR1/3/5 protein translated from the mRNA in the critical and recovery patients and mice, samples of human CSF and mouse brain tissues were collected. Neutrophils were isolated from the samples. Proteins were separated by SDS-PAGE followed by Western blot analysis. After probing with primary antibodies in TBST(TBS+ 0.1% Tween20) + 2.5% BSA overnight at 4°C, blots were incubated with secondary antibodies in TBST + 0.5% BSA for 1 h at RT.

Deep sequencing and data analysis

Deep sequencing was performed by ABLife (Wuhan, China) to identify miRNAs related to EV71 infection and host response using diseased and healthy samples of human neutrophils from CSF and blood and of mouse brain tissues. The ABLife bioinformatics group performed all related data analysis and carried out verification experiments using qRT-PCR. In brief, neutrophils were isolated from brain tissues of WT and EV71-infected mice or from CSF samples of severe patients at the acute (critical) and recovered phases.Total miRNA was extracted from the neutrophils using the mirVana miRNA isolation kit according to the manu- facturer's protocol (ThermoFisher Scientific, Carlsbad, USA), until the quality and the concentration of the RNA samples were fit for the next step. The miRNA sequencing library construction followed standard procedure of SOLiD small RNA expression kit (ThermoFisher Scientific). All SOLiD run parameters followed standard protocols. Different barcodes were introduced to two samples in the polymerase chain reaction of library construction, and all the samples were sequenced in a single sequencing run. SOLiD data were first analyzed by SOLiDSystem Small RNA Analysis Pipeline Tool (RNA2MAP).The miRbase sequences being were downloaded from miRBase (http://www.mirbase.org/). The number of bases to use when generating initial seeds locations was 18 with a tolerance of 3 mismatches. After extension step, at most 6 mismatches were allowed in full length mapping. Potential conserved target genes of differentially expressed miRNAs were firstly predicted by targetscan (http://www.targetscan.org/). Target genes of some miRNAs which could not be predicted in targetscan database, we further predicted those miRNAs targets using miRanda (http://www.microrna.org/microrna/home.do). We firstly used the Z test to determine the statistical significance of the differences between them. This approach is to look at the number of copies of a specic miRNA per cell as a fraction or proportion of the total number of miRNA molecules.

miRNAs were considered significantly altered only when they full led three criteria: (1) having at least 10 copies by SOLiD sequencing, (2) mean fold change >2 or <0.5,and (3) *Z* score > 1.96 or< −1.96.

3′-UTR cloning and luciferase reporter assay

The miRNAs targeting CCL-3 in human (GenBank No. NM_002983.2) or C57BL/6 mouse (GenBank No. NM_011337.2) were validated by cloning the complete 3′-UTRs of each and subjecting to luciferase reporter assay. Briefly, RiboBio Co., Inc. was contracted to PCR amplify the 3'-UTR sequence fragments (for human, 413bp; for mouse, 409bp) using primers to introduce restriction sites for XhoI and NotI (for cloning into the pmiR-RB-Report vector; RiboBio Co., Ltd) and to introduce mutations in the miRNA binding sites. Primers used for generation of 3′-UTR luciferase reporter constructs are shown in Table S3. Sequencing was performed to verify the correct alignment of all recombinant constructs.

In our laboratory, luciferase reporter assays were carried out by co-transfecting 293T cells (ATCC, Manassas, VA, USA) with the various pmiR-RB-Report constructs and miRNAs (40 nm concentration) using RiboFECT CP (RiboBio Co., Ltd). Thirty-six hours after transfection, luciferase activity was measured using the Dual-Luciferase Reporter Assay System (Promega Corp., Madison, WI, USA). Total renilla luciferase activity was calculated by normalizing to firefly luciferase in order to correct for differences in transfection efficiency.

QUANTIFICATION AND STATISTICAL ANALYSIS

All experiments were performed at least twice. Time courses were analyzed by repeated measurements (mixed model) ANOVA with Bonferroni post *t*-tests. Survival data were analyzed by Kaplan-Meier survival analysis. Differences in qRT-PCR data were assessed using ANOVA and Student's *t*-test. The cell type assessment was carried out by FACSCalibur™ flow cytometer equipped with CellQuest™ analysis software (BD Biosciences). Each cell type count was expressed as percentage of the total BIL cell count. miRNAs were considered significantly altered only when they full led three criteria: (1) having at least 10 copies by SOLiD sequencing, (2) mean fold change >2 or <0.5,and (3) *Z* score > 1.96 or< −1.96. The array analyses of Cytokine and chemokine measurement were performed using the Bio-Plex® 200 Protein Array System (Bio-Rad).

All data are expressed as mean ± SEM. The quantitative cytokine/chemokine profiles were compared by Mann-Whitney *U* test. Measurements at single time points were analyzed by unpaired *t*-test or analysis of variance (ANOVA) with two-tailed *t*-test. All statistical tests were calculated using the GraphPad Prism 8.0 program (GraphPad Software, Inc., San Diego, CA).